ELSEVIER

Chemical Geology 164 (2000) 1–20

CHEMICAL GEOLOGY
INCLUDING
ISOTOPE GEOSCIENCE

www.elsevier.com/locate/chemgeo

# Salts of aliphatic carboxylic acids: Raman spectra and ion pairing in hydrothermal solutions containing sodium and calcium acetates

John D. Frantz *

*Geophysical Laboratory, Carnegie Institution of Washington, Washington, DC 20015-1305, USA*

Received 26 May 1998; accepted 28 May 1999

**Abstract**

A 2.0 molal solution of sodium acetate and 0.1, 0.5, and 1.0 molal solutions of calcium acetate were investigated by Raman spectroscopy from 22 to 400°C at 1000 and 2000 bar. Experiments were performed in a special hydrothermal pressure vessel fitted with conical diamond windows. In the case of the sodium acetate solution, perturbations of the internal vibrational modes of the acetate ligand resulting from the formation of sodium acetate ion pairs were undetectable. In the case of calcium acetate, however, the OCO bending mode, the C–C symmetric stretching mode, and the C–O symmetric stretching mode all showed evidence of ion pairing between calcium and acetate. The degree of formation of the ion pairs increased with increasing temperature, increasing concentration, and decreasing pressure. Mass action constants were calculated for the reaction involving $Ca^{2+}$, $CH_3COO^-$, and $CaCH_3COO^+$ which compare favorably with theoretically derived constants and with values derived from solubility experiments. The solutions existed metastably until temperatures approaching 480°C at which the acetate ligands underwent decarboxylation resulting in the formation of bicarbonate and methane. Combining mass action constants derived from this study with constants derived from the literature, distributions of the aqueous species were computed for the experimental conditions of the spectral measurements. 

*Keywords:* Raman spectroscopy; Acetate; Hydrothermal

## 1. Introduction

The presence of organic acids under subsurface conditions has been documented by its association with oil-field brines at temperatures approaching 200°C and the association of condensed organic material with sedimentary ore deposits which formed hydrothermally at temperatures up to 250°C (Giordano, 1993; Shock, 1993). Of the saturated acyclic aliphatic monocarboxylic acids and their associated salts, acetates, propanoates, and butanoates have been shown to be the most abundant in oil-field brines at temperatures above 100°C (Sverjensky, 1984). These acids are, however, metastable under subsurface conditions reacting with the breaking of the carbon–carbon bond (decarboxylation) to form carbon dioxide and methane (Kharaka et al., 1983). Palmer and Drummond (1986), in their study of thermal decarboxylation of acetate, studied the kinet-

* Fax: +1-202-686-2419; e-mail: frantz@gl.ciw.edu

0009-2541/00/$ - see front matter 
PII: S0009-2541(99)00137-0

ics of decarboxylation and the role of catalysis. Their results interpreted by Drummond and Palmer (1986) demonstrated that ''acetate can survive moderate hydrothermal temperatures ($< 300$°C) long enough to promote mobility of metals as acetate complexes.'' It is, therefore, important to consider the presence of aliphatic acids and their associated salts in modeling subsurface hydrothermal fluids associated with organic material.

Considerable attention has been given towards the experimental determination of the relative stabilities of acetate complexes under hydrothermal temperatures and pressures. Palmer and Drummond (1988) used potentiometric methods in their study of stability constants of ferrous acetate complexes at elevated temperatures and pressures. Ellis (1963) determined the ionization of acetic acid from conductance measurements to 225°C. Speciation in solutions containing acetic acid were studied to 275°C at 90 bar using Raman spectroscopy by Semmler and Irish (1988). Semmler et al. (1990) investigated complexing in magnesium acetate solutions to 250°C at 90 bar. Yang et al. (1989) spectroscopically identified lead and zinc acetate complexes in solutions at temperatures to 250°C and pressures to 110 bar. Giordano (1989) determined stability constants for lead acetate complexes to 85°C in his lead sulfate solubility studies. Seewald and Seyfried (1991) in their study of the solubility of portlandite in acetate solutions from 100 to 350°C at 500 bar retrieved stability constants for $CaCH_3COO^+$ from solubility data. Shock and Koretsky (1993) estimated the thermodynamic properties of acetate complexes and their relative stabilities based on existing experimental data and correlation algorithms.

The present study focuses on the determination of the behavior of sodium and calcium acetate solutions as a function of temperature and pressure. As in the case of Yang et al. (1989) and Semmler et al. (1990), Raman spectroscopy is used both to identify com-

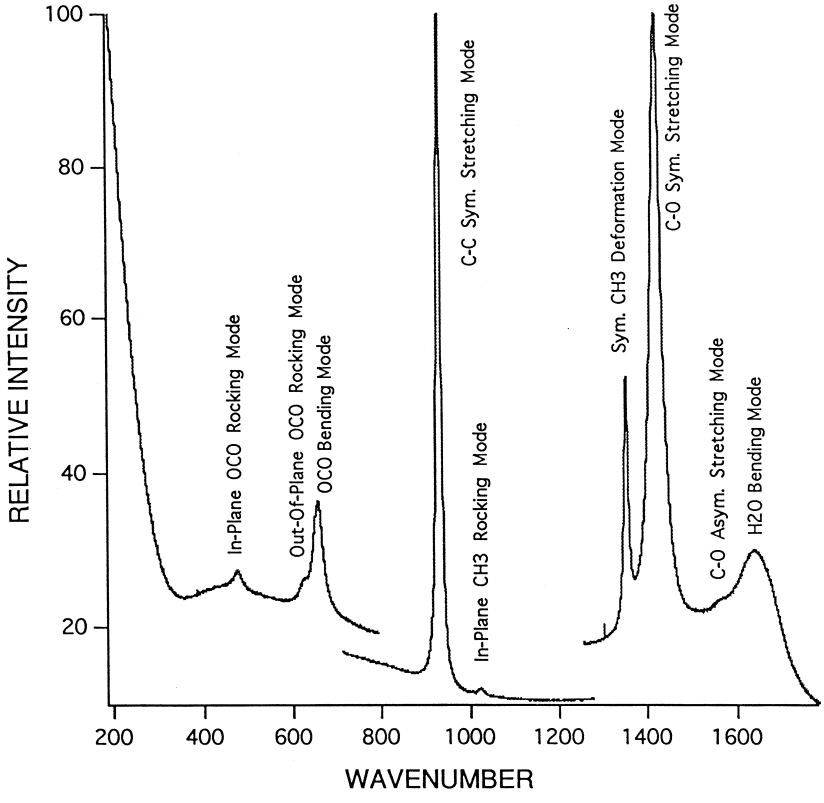


Fig. 1. Raman spectra of a 2 molal sodium acetate solution at 25°C and 1 atm. Not shown are the $CH_3$ symmetric and asymmetric stretching modes occurring at frequencies between 2900 and 3000 $cm^{-1}$.

plexes and determine mass action constants describing their relative concentrations. The behavior of calcium acetate solutions is of particular interest due to the influence that acetate potentially has on the chemistry of carbonate fluids determining the stability of carbonate cements (i.e., calcite) in sedimentary basins and on the chemistry of ore-forming hydrothermal fluids.

## 2. Experimental methods

The Raman spectra of sodium and calcium-bearing aqueous solutions were collected using a specially designed hydrothermal pressure vessel with diamond windows (Frantz, 1981; Frantz et al., 1993). The disk-shaped pressure vessel (diameter: 2 in.; height: 1 in.) contains two conical low-fluorescence diamond windows set at right angles to one another. The cell, containing a $Pt–Pt_{90}Rh_{10}$ thermocouple extending into the fluid cavity, is heated using two spirally wound platinum resistance furnace elements. The fluid is introduced and pressure is generated using a small stainless-steel intensifier. Pressure is measured using an Autoclave® 0–60,000 psi transducer. Pressure calibration of the transducer was accomplished using a recently calibrated Heise® bourdin-tube gauge. A melting point furnace was

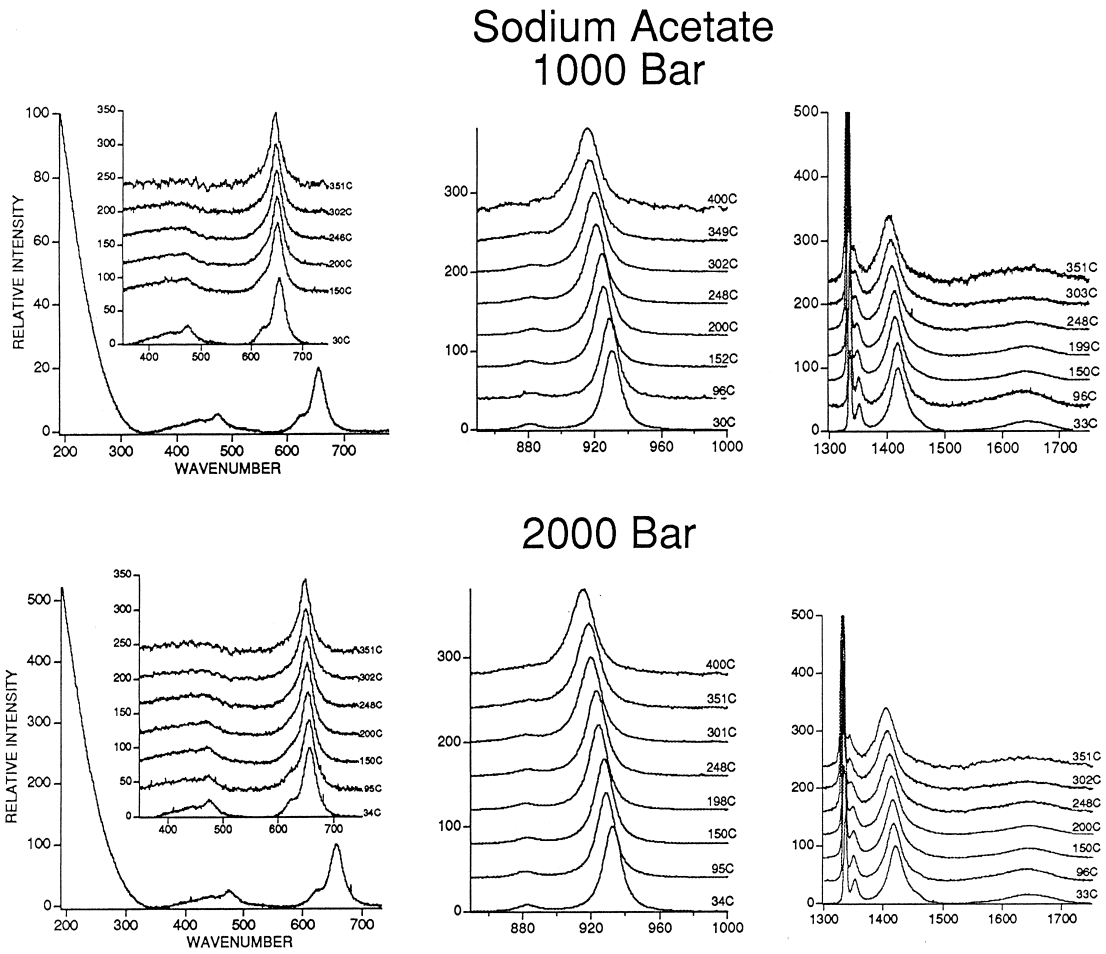


Fig. 2. Raman spectra of a 2 molal sodium acetate solution as a function of temperature (°C) at pressures of 1000 and 2000 bar. Three spectral ranges are shown.

Table 1
Results of deconvolutions

*1.0 Molal Calcium Acetate Solution (1000 Bar)*

| 192–792 range | Temp (°C) | Freq(1) | Area(1) | Width(1) | Freq(2) | Area(2) | Width(2) | Freq(3) | Area(3) | Width(3) |
|---|---|---|---|---|---|---|---|---|---|---|
| | 22 | 621.1 | 122 | 21.4 | 655.8 | 576 | 28.1 | 675.6 | 91 | 18.0 |
| | 96 | 623.0 | 101 | 24.1 | 654.8 | 455 | 28.4 | 674.6 | 88 | 16.1 |
| | 145 | 623.4 | 94 | 27.9 | 653.5 | 359 | 28.0 | 673.4 | 120 | 20.2 |
| | 199 | 628.6 | 133 | 44.5 | 653.0 | 214 | 26.9 | 671.8 | 88 | 17.6 |
| | 249 | 631.0 | 140 | 63.1 | 650.7 | 96 | 24.4 | 670.0 | 77 | 20.0 |

| 710–1275 range | Temp (°C) | Freq(4) | Area(4) | Width(4) | Freq(5) | Area(5) | Width(5) | Freq(6) |
|---|---|---|---|---|---|---|---|---|
| | 24 | 936.0 | 1263 (43) | 12.5 | 942.8 | 524 (45) | 11.7 | na |
| | 53 | 935.4 | 1252 (28) | 13.0 | 942.9 | 647 (28) | 11.6 | na |
| | 79 | 934.6 | 1158 (24) | 13.2 | 942.4 | 707 (24) | 11.8 | na |
| | 98 | 933.7 | 1177 (27) | 13.6 | 941.8 | 857 (27) | 12.4 | na |
| | 130 | 932.5 | 620 | 14.2 | 941.0 | 654 | 13.1 | na |
| | 163 | 931.2 | 576 | 14.7 | 940.1 | 580 | 14.2 | na |
| | 189 | 930.1 | 489 | 16.0 | 939.2 | 562 | 14.7 | na |
| | 248 | 922.5 | 217 | 18.1 | 932.3 | 321 | 14.1 | 942.9 |
| | 302 | 921.3 | 107 | 23.5 | 931.5 | 201 | 15.0 | 942.5 |
| | 352 | 917.7 | 63 | 33.5 | 929.4 | 96 | 15.6 | 940.2 |

| 1254–1783 range | Temp (°C) | Freq(7) | Freq(8) | Freq(9) | Area(9) | Width(9) | Freq(10) | Area(10) | Width(10) |
|---|---|---|---|---|---|---|---|---|---|
| | 22 | 1335.5 | 1352.2 | 1419.9 | 3470 | 30.9 | 1442.5 | 827 | 33.2 |
| | 96 | 1335.8 | 1352.8 | 1419.4 | 1859 | 33.9 | 1442.5 | 637 | 38.6 |
| | 145 | 1333.9 | 1351.2 | 1416.6 | 1080 | 35.9 | 1439.4 | 490 | 40.4 |
| | 198 | 1333.8 | 1351.1 | 1415.2 | 490 | 37.5 | 1437.3 | 361 | 43.2 |
| | 248 | 1331.7 | 1349.9 | 1412.6 | 245 | 40.4 | 1434.7 | 291 | 49.2 |

*1.0 Molal Calcium Acetate Solution (2000 Bar)*

| 192–792 range | Temp (°C) | Freq(1) | Area(1) | Width(1) | Freq(2) | Area(2) | Width(2) | Freq(3) | Area(3) | Width(3) |
|---|---|---|---|---|---|---|---|---|---|---|
| | 28 | 621.1 | 114 | 20.4 | 656.6 | 672 | 28.2 | 675.6 | 89 | 18.6 |
| | 96 | 622.1 | 102 | 24.6 | 655.3 | 554 | 28.7 | 675.0 | 89 | 16.9 |
| | 145 | na | na | na | 653.6 | 370 | 23.8 | 671.9 | 104 | 16.7 |
| | 200 | na | na | na | 653.1 | 285 | 26.6 | 672.3 | 92 | 18.1 |
| | 248 | 623.5 | 81 | 51.2 | 651.9 | 191 | 30.0 | 671.8 | 73 | 19.8 |
| | 303 | 622.1 | 38 | 51.6 | 649.0 | 97 | 28.7 | 670.2 | 66 | 24.0 |

| 710–1275 range | Temp (°C) | Freq(4) | Area(4) | Width(4) | Freq(5) | Area(5) | Width(5) | Freq(6) |
|---|---|---|---|---|---|---|---|---|
| | 24 | 936.9 | 1370 (49) | 13.0 | 943.4 | 436 (50) | 11.8 | na |
| | 53 | 936.3 | 1358 (32) | 13.4 | 943.4 | 591 (31) | 11.6 | na |
| | 75 | 935.7 | 1331 (29) | 13.4 | 943.1 | 664 (28) | 11.7 | na |
| | 98 | 934.6 | 1331 (27) | 13.6 | 942.4 | 753 (26) | 11.9 | na |
| | 129 | 933.7 | 831 (20) | 14.3 | 941.9 | 637 (21) | 12.4 | na |
| | 163 | 932.3 | 721 | 14.8 | 940.9 | 742 | 13.4 | na |
| | 190 | 931.1 | 597 | 15.4 | 940.0 | 577 | 14.3 | na |
| | 248 | 924.2 | 263 | 17.3 | 933.8 | 423 | 15.6 | na |
| | 304 | 921.7 | 175 | 19.7 | 931.7 | 268 | 14.4 | 942.2 |
| | 350 | 920.3 | 103 | 25.8 | 931.0 | 157 | 15.0 | 942.0 |

Table 1 (continued)

*1.0 Molal Calcium Acetate Solution (2000 Bar)*

| 1254–1783 range | Temp (°C) | Freq(7) | Freq(8) | Freq(9) | Area(9) | Width(9) | Freq(10) | Area(10) | Width(10) |
|---|---|---|---|---|---|---|---|---|---|
| | 28 | 1335.7 | 1352.7 | 1420.3 | 3448 | 30.2 | 1441.6 | 989 | 35.7 |
| | 98 | 1334.8 | 1351.9 | 1418.8 | 2207 | 33.0 | 1441.6 | 661 | 36.4 |
| | 144 | 1335.0 | 1352.3 | 1418.1 | 1321 | 35.0 | 1440.5 | 533 | 39.2 |
| | 199 | 1333.0 | 1350.5 | 1415.0 | 712 | 38.0 | 1437.1 | 418 | 43.0 |

*0.1 Molal Calcium Acetate Solution (1000 Bar)*

| 710–1275 range | Temp (°C) | Freq(4) | Area(4) | Width(4) | Freq(5) | Area(5) | Width(5) | Freq(6) |
|---|---|---|---|---|---|---|---|---|
| | 28 | 936.8 | 1087 | 13.4 | na | na | na | na |
| | 52 | 936.1 | 1058 | 13.7 | na | na | na | na |
| | 74 | 935.2 | 1000 | 13.8 | 944.3 | 27 | 6.9 | na |
| | 99 | 934.2 | 744 | 13.6 | 943.5 | 40 | 7.5 | na |
| | 121 | 932.5 | 515 (15) | 13.9 | 942.1 | 54 (9) | 8.8 | na |
| | 151 | 931.3 | 333 (11) | 14.2 | 941.4 | 85 (10) | 9.6 | na |
| | 179 | 930.1 | 265 (12) | 14.8 | 940.4 | 78 (9) | 10.6 | na |
| | 199 | 929.3 | 242 (12) | 16.8 | 940.0 | 64 (6) | 9.5 | na |
| | 230 | 927.2 | 118 (16) | 19.1 | 938.3 | 106 (28) | 12.6 | na |
| | 253 | 926.0 | 115 | 20.4 | 937.2 | 135 | 13.1 | na |

*0.1 Molal Calcium Acetate Solution (2000 Bar)*

| 710–1275 range | Temp (°C) | Freq(4) | Area(4) | Width(4) | Freq(5) | Area(5) | Width(5) | Freq(6) |
|---|---|---|---|---|---|---|---|---|
| | 28 | 937.7 | 971 | 13.6 | na | na | na | na |
| | 50 | 937.1 | 957 | 14.0 | na | na | na | na |
| | 72 | 936.2 | 888 | 14.2 | na | na | na | na |
| | 94 | 935.5 | 674 | 14.6 | na | na | na | na |
| | 121 | 933.8 | 480 (15) | 15.2 | 943.7 | 30 (9) | 8.2 | na |
| | 152 | 932.5 | 363 (9) | 14.8 | 943.1 | 35 (4) | 7.0 | na |
| | 179 | 931.2 | 260 (15) | 15.2 | 941.6 | 88 (16) | 9.5 | na |
| | 200 | 930.3 | 205 (10) | 16.6 | 941.0 | 62 (9) | 9.7 | na |
| | 231 | 928.7 | 159 (21) | 18.6 | 939.7 | 87 (31) | 9.5 | na |
| | 253 | 927.4 | 87 (14) | 20.7 | 938.1 | 62 (11) | 11.2 | na |

*0.5 Molal Calcium Acetate Solution (1000 Bar)*

| 710–1275 range | Temp (°C) | Freq(4) | Area(4) | Width(4) | Freq(5) | Area(5) | Width(5) | Freq(6) |
|---|---|---|---|---|---|---|---|---|
| | 24 | 936.5 | 1891 | 14.5 | na | na | na | na |
| | 50 | 934.5 | 1397 (30) | 12.7 | 941.8 | 449 (30) | 10.7 | na |
| | 73 | 933.8 | 1470 (21) | 12.9 | 941.6 | 406 (19) | 10.5 | na |
| | 104 | 932.9 | 1120 (15) | 13.3 | 941.2 | 415 (14) | 10.7 | na |
| | 128 | 931.8 | 996 (14) | 13.8 | 940.6 | 446 (12) | 11.3 | na |
| | 152 | 930.7 | 761 (13) | 13.8 | 939.7 | 523 (13) | 11.8 | na |
| | 175 | 929.7 | 625 (12) | 14.5 | 939.0 | 529 (12) | 12.4 | na |
| | 200 | 928.7 | 448 | 15.1 | 938.4 | 482 | 12.9 | na |
| | 226 | 927.6 | 384 | 15.8 | 937.6 | 383 | 13.8 | na |
| | 250 | 926.2 | 247 | 16.6 | 936.7 | 328 | 14.8 | na |

*0.5 Molal Calcium Acetate Solution (2000 Bar)*

| 710–1275 range | Temp (°C) | Freq(4) | Area(4) | Width(4) | Freq(5) | Area(5) | Width(5) | Freq(6) |
|---|---|---|---|---|---|---|---|---|
| | 25 | 937.2 | 1914 | 14.4 | na | na | na | na |
| | 49 | 936.5 | 1502 (31) | 15.0 | 942.0 | 409 (31) | 12.6 | na |

Table 1(continued)

*1.0 Molal Calcium Acetate Solution (2000 Bar)*

| 710–1275 range | Temp (°C) | Freq(4) | Area(4) | Width(4) | Freq(5) | Area(5) | Width(5) | Freq(6) |
|---|---|---|---|---|---|---|---|---|
| | 72 | 934.8 | 1468 (22) | 13.1 | 942.1 | 399 (21) | 10.4 | na |
| | 104 | 933.8 | 1256 (16) | 13.4 | 941.7 | 368 (14) | 10.6 | na |
| | 127 | 932.9 | 1098 (16) | 13.7 | 941.2 | 410 (14) | 10.9 | na |
| | 152 | 931.9 | 937 (14) | 14.1 | 940.6 | 443 (13) | 11.4 | na |
| | 175 | 931.0 | 808 (12) | 14.7 | 939.9 | 445 (11) | 11.7 | na |
| | 201 | 929.8 | 640 (14) | 15.1 | 939.1 | 492 (13) | 12.5 | na |
| | 224 | 928.7 | 439 | 15.6 | 938.4 | 473 | 12.9 | na |
| | 250 | 927.6 | 398 | 16.4 | 937.6 | 357 | 13.7 | na |

*2.0 Molal Sodium Acetate Solution (1000 Bar)*

| 192–792 range | Temp (°C) | Freq(1) | Area(1) | Width(1) | Freq(2) | Area(2) | Width(2) |
|---|---|---|---|---|---|---|---|
| | 30 | 620.9 | 71 | 21.9 | 655.1 | 533 | 26.4 |
| | 97 | na | na | na | 653.5 | 409 | 28.1 |
| | 150 | 621.2 | 65 | 27.9 | 651.4 | 503 | 25.9 |
| | 200 | 623.6 | 65 | 32.1 | 651.2 | 453 | 25.5 |
| | 246 | 623.9 | 73 | 41.5 | 650.0 | 403 | 25.0 |
| | 302 | 624.0 | 86 | 57.1 | 648.6 | 300 | 23.4 |
| | 351 | na | na | na | 646.8 | 158 | 22.5 |

| 710–1275 range | Temp (°C) | Freq(4) | Width(4) |
|---|---|---|---|
| | 30 | 930.2 | 12.3 |
| | 96 | 928.7 | 12.0 |
| | 152 | 925.0 | 12.4 |
| | 200 | 924.2 | 13.0 |
| | 248 | 920.5 | 13.8 |
| | 302 | 919.3 | 15.1 |
| | 349 | 916.3 | 15.6 |
| | 400 | 915.2 | 16.9 |

| 1254–1783 range | Temp (°C) | Freq(7) | Freq(8) | Area(8) | Width(8) | Freq(9) | Area(9) | Width(9) |
|---|---|---|---|---|---|---|---|---|
| | 33 | 1335.4 | 1351.4 | 444 | 10.5 | 1418.4 | 2926.4 | 29.0 |
| | 96 | 1335.6 | 1351.7 | 192 | 9.6 | 1417.0 | 1349.0 | 29.1 |
| | 150 | 1333.3 | 1349.6 | 155 | 10.3 | 1412.8 | 1264.8 | 32.7 |
| | 199 | 1333.8 | 1349.9 | 99 | 9.2 | 1412.1 | 1090.3 | 36.5 |
| | 248 | 1331.6 | 1347.7 | 76 | 9.6 | 1408.1 | 891.6 | 39.0 |
| | 303 | 1331.8 | 1346.1 | 82 | 11.7 | 1406.2 | 755.8 | 38.6 |
| | 351 | 1329.3 | 1343.4 | 34 | 10.0 | 1402.9 | 398.1 | 40.7 |
| | 400 | 1329.4 | 1343.9 | 3 | 4.1 | 1406.5 | 123.1 | 53.9 |

*2.0 Molal Sodium Acetate Solution (2000 Bar)*

| 192–792 range | Temp (°C) | Freq(1) | Area(1) | Width(1) | Freq(2) | Area(2) | Width(2) |
|---|---|---|---|---|---|---|---|
| | 34 | 620.7 | 73 | 22.4 | 656.2 | 563 | 27.3 |
| | 95 | 622.2 | 115 | 38.1 | 654.7 | 505 | 26.5 |
| | 150 | 622.7 | 74 | 30.4 | 653.1 | 490 | 26.3 |
| | 200 | 623.2 | 78 | 36.9 | 651.9 | 444 | 25.9 |
| | 248 | 623.3 | 57 | 36.5 | 651.1 | 416 | 25.4 |
| | 302 | 624.3 | 64 | 49.9 | 649.9 | 326 | 24.9 |
| | 351 | na | na | na | 648.1 | 219 | 24.5 |
| | 400 | na | na | na | 645.8 | 100 | 23.2 |

Table 1(continued)

*1.0 Molal Calcium Acetate Solution (1000 Bar)*

| 710–1275 range | Temp (°C) | Freq(4) | Width(4) |
|---|---|---|---|
| | 34 | 932.2 | 12.4 |
| | 95 | 928.5 | 12.2 |
| | 150 | 927.3 | 12.5 |
| | 198 | 924.0 | 13.1 |
| | 248 | 922.8 | 13.9 |
| | 301 | 919.4 | 14.8 |
| | 351 | 918.2 | 15.5 |
| | 400 | 914.7 | 16.7 |

| 1254–1783 range | Temp (°C) | Freq(7) | Freq(8) | Area(8) | Width(8) | Freq(9) | Area(9) | Width(9) |
|---|---|---|---|---|---|---|---|---|
| | 33 | 1336.5 | 1352.9 | 332 | 9.7 | 1419.9 | 2375 | 28.5 |
| | 96 | 1334.5 | 1350.9 | 238 | 9.6 | 1416.7 | 1888 | 30.2 |
| | 150 | 1334.7 | 1351.4 | 155 | 10.2 | 1415.1 | 1319 | 32.8 |
| | 200 | 1334.1 | 1350.9 | 146 | 11.8 | 1412.5 | 1017 | 33.5 |
| | 248 | 1332.6 | 1349.5 | 72 | 10.6 | 1410.1 | 829 | 41.1 |
| | 302 | 1330.7 | 1345.6 | 95 | 11.9 | 1406.0 | 841 | 38.9 |
| | 351 | 1330.5 | 1345.0 | 52 | 11.4 | 1404.6 | 511 | 40.3 |
| | 400 | 1328.4 | 1343.8 | 13 | 8.0 | 1401.8 | 197 | 42.2 |

Where: Peak(1): Out-of-Plane OCO rocking mode, Peak(2): OCO bending mode (unbound acetate), Peak(3): OCO bending mode (bound acetate), Peak(4): C–C symmetric stretching mode (unbound acetate), Peak(5): C–C symmetric stretching mode (bound acetate), Peak(6): C–C symmetric stretching mode (bound acetate), Peak(7): C–C symmetric stretching mode (diamond), Peak(8): symmetric $CH_3$ deformation mode, Peak(9): symmetric C–O stretching mode (unbound acetate), Peak(10): symmetric C–O stretching mode (bound acetate).

used in the temperature calibration of the thermocouples. Temperature errors are thought to be $\pm 5$°C; pressure errors, $\pm 10$ bar. The pressure vessel and much of the pressure-generating apparatus are gold plated to reduce the effects of corrosion and therefore inhibit fluorescence. Prior to use, the cell and associated pressure-generating apparatus were repeatedly cleaned with ultra-pure hexane, methanol, and triple-distilled water. Great care was taken in filling the system with the sample fluid in order to prevent the introduction of dust and bubbles.

The optical cell was used in conjunction with a Dilor® XY confocal Raman spectrometer equipped with CCD detector. Gratings with 1800 lines/mm yield a spectral resolution of approximately 1 $cm^{-1}$. The 514.5 nm line of a SpectroPhysics® model 2025 $Ar^+$ laser operating at 1.8 W was used for sample excitation. The spectrometer was calibrated with respect to wavenumber using both the frequency of the laser line and a mercury lamp. Collection of the scattered light was at 90° to the incident radiation. Experiments were performed by first incrementing temperature and measuring spectra at varying pressures. Signal collection times averaged 300 s. Analyses of the resulting Raman spectra were accomplished using computer algorithms contained in the software package *Igor Pro* (WaveMetrics®).

The 2.0 molal sodium acetate aqueous solution was prepared from crystalline anhydrous sodium acetate reagent (Alfa®, Stock #11554, Lot #F13G02) and doubly distilled water; the 0.1, 0.5, and 1.0 molal calcium acetate solutions, from hydrous calcium acetate powder (Alfa®, Stock #13446, Lot #082180). The solutions used in the experiments were prepared by mixing solutions with concentrations higher than those desired, performing sodium or calcium analyses of these using atomic absorption spectrometry, and diluting these to the desired molality.

## 3. Spectral assignments

Acetate, an acyclic aliphatic framework molecule, is composed of a carboxyl group and a single methyl

group. As an unbound aqueous ligand, the acetate ion exhibits $C_{2v}$ symmetry with 15 vibrational modes (Kaklhana et al., 1983). The primary modes of the carboxyl group are the OCO in-plane rocking mode ($\gamma_{in(OCO)}$), the OCO out-of-plane rocking mode ($\pi_{(OCO)}$), the OCO in-plane bending mode ($\delta_{(OCO)}$), and the symmetric ($\nu_{s(CO)}$) and antisymmetric ($\nu_{as(CO)}$) C–O symmetric stretching modes. The methyl group exhibits a symmetric ($\nu_{s(CH_3)}$) and asymmetric ($\nu_{as(CH_3)}$) $CH_3$ stretching mode, a $CH_3$ stretching mode ($\nu_{(CH_3)}$), in- ($\gamma_{in(CH_3)}$) and out-of-plane ($\pi_{(CH_3)}$) $CH_3$ rocking modes, symmetric ($\delta_{s(CH_3)}$) and asymmetric ($\delta_{as(CH_3)}$) deformation modes, an additional deformation mode ($\delta_{(CH_3)}$) and a torsion mode ($\tau_{(CH_3)}$). The C–C symmetric stretching mode ($\nu_{(C-C)}$) represents a fundamental vibrational mode resulting from the interaction of the carboxyl and methyl groups. Of these modes, only eight are discernible in our Raman spectra of a 2 molal solution of sodium acetate collected between 192 and 1783 $cm^{-1}$ at 25°C, 1 atm (Fig. 1). The in-plane OCO rocking mode occurs at 476 $cm^{-1}$; the out-of-plane OCO rocking mode, at 628 $cm^{-1}$; the OCO in-plane bending mode, at 657 $cm^{-1}$; the C–C symmetric stretching mode, at 931 $cm^{-1}$; the $CH_3$ in-plane rocking mode, at 1023 $cm^{-1}$; the $CH_3$ symmetric deformation mode, at 1352 $cm^{-1}$; the C–O symmetric stretching mode, at 1419 $cm^{-1}$; and the C–O asymmetric stretching mode at 1561 $cm^{-1}$. The out-of-plane $CH_3$ rocking mode is indiscernible. The asymmetric $CH_3$ deformation mode is obscured by the C–O symmetric stretching mode.

The association of cations with complex ligands can occur as solvent-separated ion pairs (outer-sphere complexes) or direct cation–anion contact pairs (inner sphere complexes). Solvent-separated ion pairs, due to the separation of the cations and anions by waters of solvation, have little effect on the Raman spectra of the complex ligand. Contact-pairs, however, do affect the internal modes of the ligand. The coordination of the association of cations with the acetate ligand as contact ion pairs (inner-sphere complexes) is difficult to assess based on the results of Raman studies without complementary X-ray and NMR studies. Possibilities include monodentate association of the cation with one oxygen, bidentate association of the cation with two oxygens, and a bridged association of two cations with the two oxygens of the carboxyl group (Yang et al., 1989). Such relatively weak associations serve to perturb the existing symmetry of the complex ligand causing existing bands to split. Due to the direct association of the cation with the carboxyl group of the acetate complex, the carboxyl vibrational modes and the mode associated with the carbon–carbon bond can be expected to most affected.

## 4. Experimental results

### *4.1. Spectroscopy*

Previous studies involving ion pairing of alkalis with complex ligands in relatively dilute solutions (Spohn and Brill, 1989; Frantz, 1998) have shown that association has undramatic, if noticeable, effects on the frequencies or half-widths of the internal modes of the ligands. This is probably due to alkalis cations primarily forming solvent-separated ion pairs. Association of alkaline earths with complex ligands (which probably form contact ion pairs due to their larger charge density), have been demonstrated to affect the internal modes of the ligands (Semmler et al., 1990; Frantz et al., 1994). In order to identify and analyze spectral perturbations due to ion-pairing, experiments were done for both sodium acetate and calcium acetate solutions.

Experiments were performed on a 2.0 molal sodium acetate solution as a function of temperature at both 1000 and 2000 bar pressure (Fig. 2). Spectra were collected in three frequency ranges: 192–792, 710–1275, and 1254–1783 $cm^{-1}$. The spectra were corrected for the Bose–Einstein effect (Long, 1977) and for background using fourth- or fifth-order polynomials. The frequencies and half-widths of the major bands are presented in Table 1 and in Fig. 3. The frequencies systematically decrease; the half-widths of the C–C symmetric stretch and the C–O symmetric stretch systematically increase with increasing temperature for both 1000 and 2000 bar. The half-widths of the OCO bending mode decrease with increasing temperature. The peak at 1330 $cm^{-1}$ (as seen in Fig. 2, corresponds to the C–C symmetric stretch of the diamond window of the optical cell. Solutions remained stable for 24-h periods with no sign of decarboxylation. Decarboxylation did occur

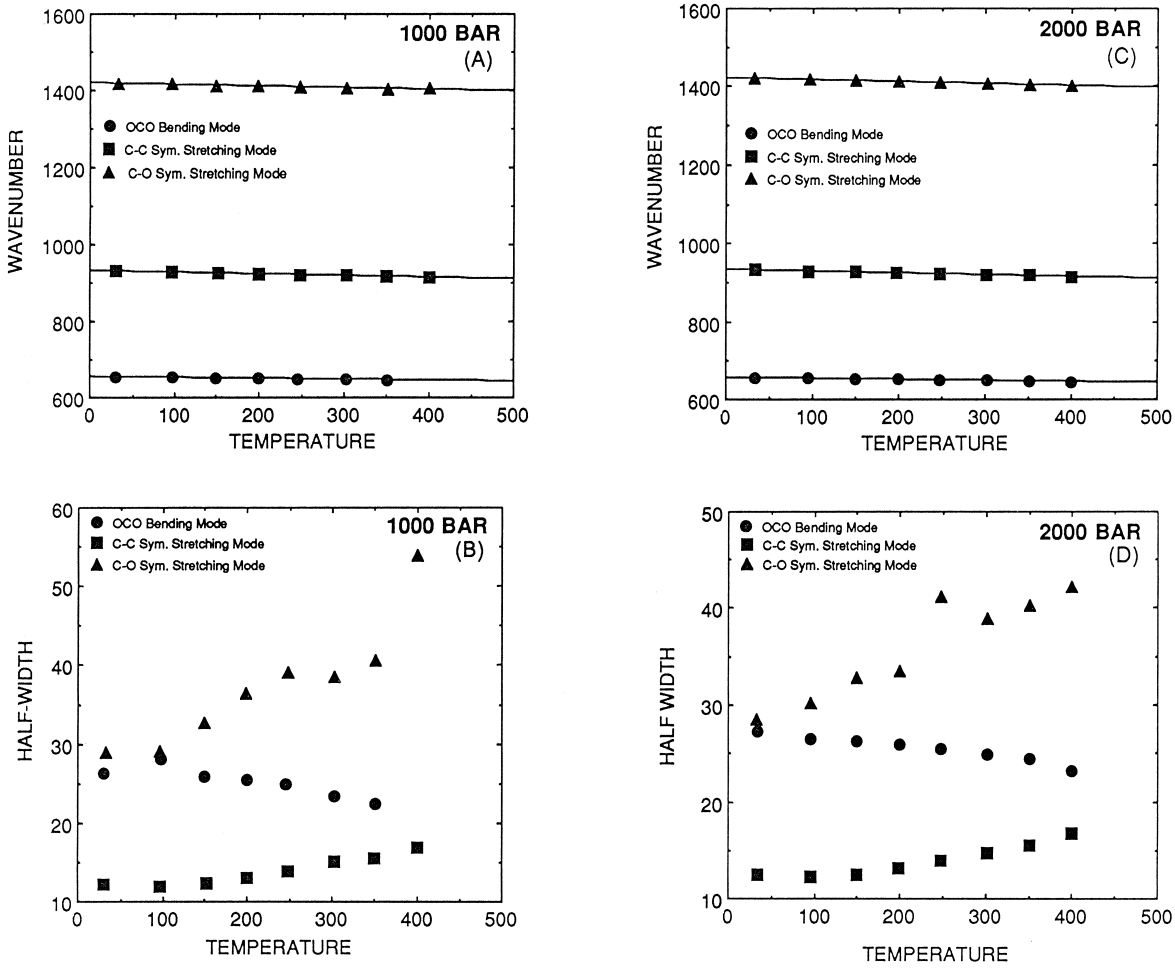


Fig. 3. Frequencies and half-widths of sodium acetate bands.

(within seconds) at approximately 480°C resulting in the appearance peaks indicating the presence of both bicarbonate and methane (Fig. 4). The spectra in Fig. 4 were taken after lowering the temperature to approximately 250°C to improve the signal to noise ratio and separate the bicarbonate peak from the acetate peak.

Experiments were carried out on 0.1, 0.5, and 1.0 molal calcium acetate solutions. The results of measurements on the 1.0 molal solution (after performing the corrections listed above) are shown in Fig. 5. Significant differences exist between the spectra of the 1.0 molal calcium acetate and the 2.0 molal sodium acetate solutions (Fig. 2). The OCO bending mode seen as a single peak in the case of sodium acetate (Fig. 2) has split into two peaks for calcium acetate with the peak at higher frequency increasing in intensity with respect to the lower frequency with increasing temperature. The C–C symmetric stretching mode identified as a single peak in the sodium acetate can be seen to have also split into two peaks again with the higher frequency peak increasing in relative intensity with respect to the lower frequency peak with increasing temperature. Similarly, the single C–O symmetric stretch shown in Fig. 2, for sodium acetate, follows the same trend. These trends were not discernible for the in- and out-of-plane rocking modes or the C–O asymmetric stretching

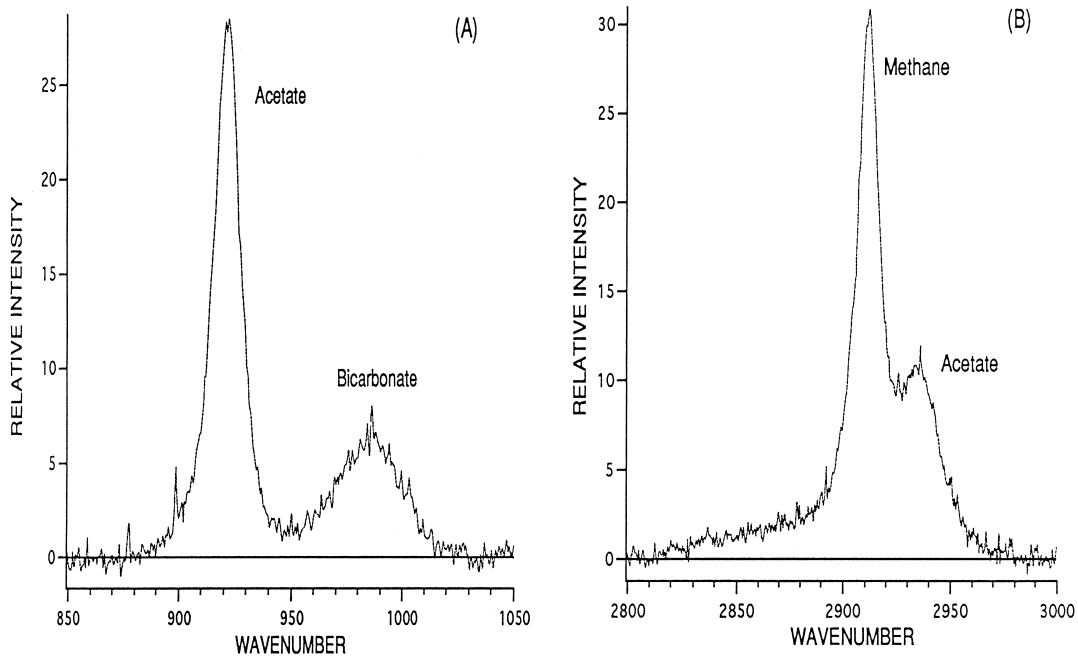


Fig. 4. Raman spectra of a 2-molal sodium acetate after decomposition at 480°C with subsequent cooling to 250°C.

mode due to their low intensities. The frequency and half-width of the symmetric $CH_3$ deformation mode is reasonably similar for both solutions and does not appear to split in the case of calcium acetate. The differences between the spectra of the 2 molal sodium acetate and the 1 molal calcium acetate solutions (both having a 2 molal concentration of the acetate ligand) are shown with the frequency ranges reduced in Fig. 6.

The spectral envelopes containing the OCO bending mode (594–712 $cm^{-1}$), the C–C symmetric stretch mode (880–988 $cm^{-1}$), and the C–O symmetric stretch mode (1310–1510 $cm^{-1}$) were deconvoluted using the software package *Igor Pro* (WaveMetrics®). In all cases, the spectral envelopes were fit using Lorenzian peak shapes with the number of bands being dictated by the inflections in the spectral envelopes. Results of the deconvolutions are presented in Table 1 and examples of these fits for calcium acetate are given in Fig. 7. Frequencies, areas and half-widths are given. In the case of the envelope containing the out-of-plane OCO rocking mode and the OCO bending mode, only three bands could be justifiably resolved. At low temperatures, the frequency of the lowest-frequency peak of the deconvolution corresponds to the out-of-plane OCO rocking mode for of the unbound acetate ligand as seen in the sodium acetate spectra. As temperature increases, however, its frequency increases rather than decreases probably indicating the presence of an unresolvable second out-of-plane OCO rocking mode band. The remaining two peaks are assigned to the OCO bending mode. Justification is based on comparison of the frequencies of the deconvoluted curves with those of sodium acetate bands (Fig. 8A,D). The frequency of the mid-frequency peak of the deconvolution for the 1 molal calcium acetate solution very closely matches that of the sodium acetate solution. The relatively high intensity of the third peak dictates that it also represents the bending mode rather than the out-of-plane rocking mode of the acetate ligand. Frequencies of the two bands representing the OCO bend systematically decrease with increasing temperature (Fig. 8A,D). Similar results can be seen from the deconvolution of the envelope containing the C–C stretch mode. The frequency of the lower

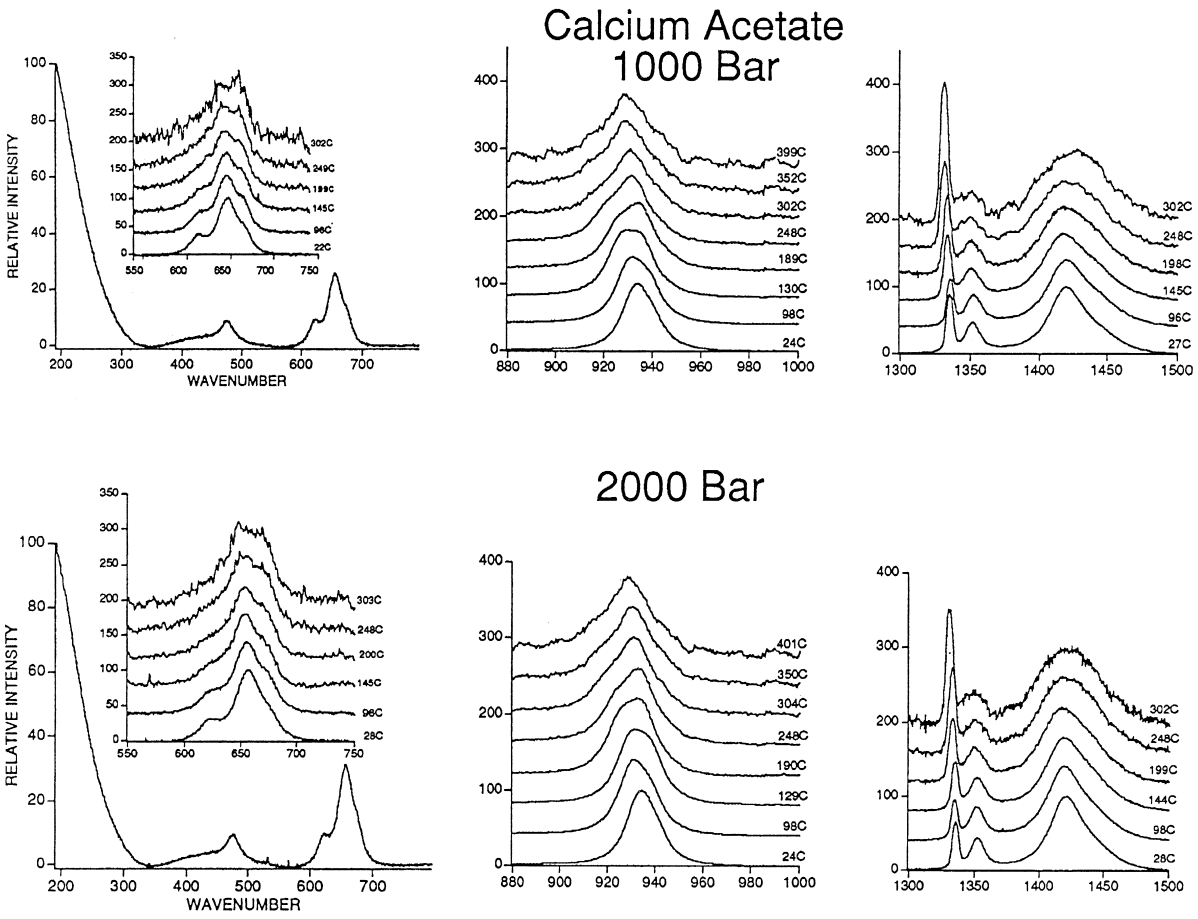


Fig. 5. Raman spectra of a 1-molal calcium acetate solution as a function of temperature (°C) at pressures of 1000 and 2000 bar. Three spectral ranges are shown.

frequency peak closely matches that of the corresponding peak of sodium acetate (Fig. 8B,E). Systematically, the frequencies of both peaks decrease and the half-widths increase with increasing temperature (Table 1). In the case of the envelope containing the C–O stretching mode, the deconvolution involved four peaks: the C–C stretch of the diamond window, the symmetric $CH_3$ deformation, and two peaks corresponding to the C–O symmetric bending mode. The frequencies for all four bands systematically decrease with increasing temperature (Table 1). The half-widths of the two peaks corresponding to the C–O stretching mode systematically increase with increasing temperature. The frequency of the lower-frequency C–C stretching mode peak matches that of sodium acetate (Fig. 8C,F).

The spectral envelope containing the C–C symmetric stretch mode contains an additional feature at higher temperatures (Fig. 9). At temperatures beginning at 248°C at 1000 bar and 304°C at 2000 bar, a third peak appears on the left-hand shoulder of the envelope. Deconvolutions of the high-temperature spectral envelopes produced three distinct peaks (Table 1). The relative intensity of this peak was found to generally increase with increasing temperature though the error was considerable due to the lower peak to background intensity ratio at the higher temperatures.

### *4.2. Chemical interpretations*

The perturbations of the internal vibrational modes of complex ligands due to interactions with aqueous

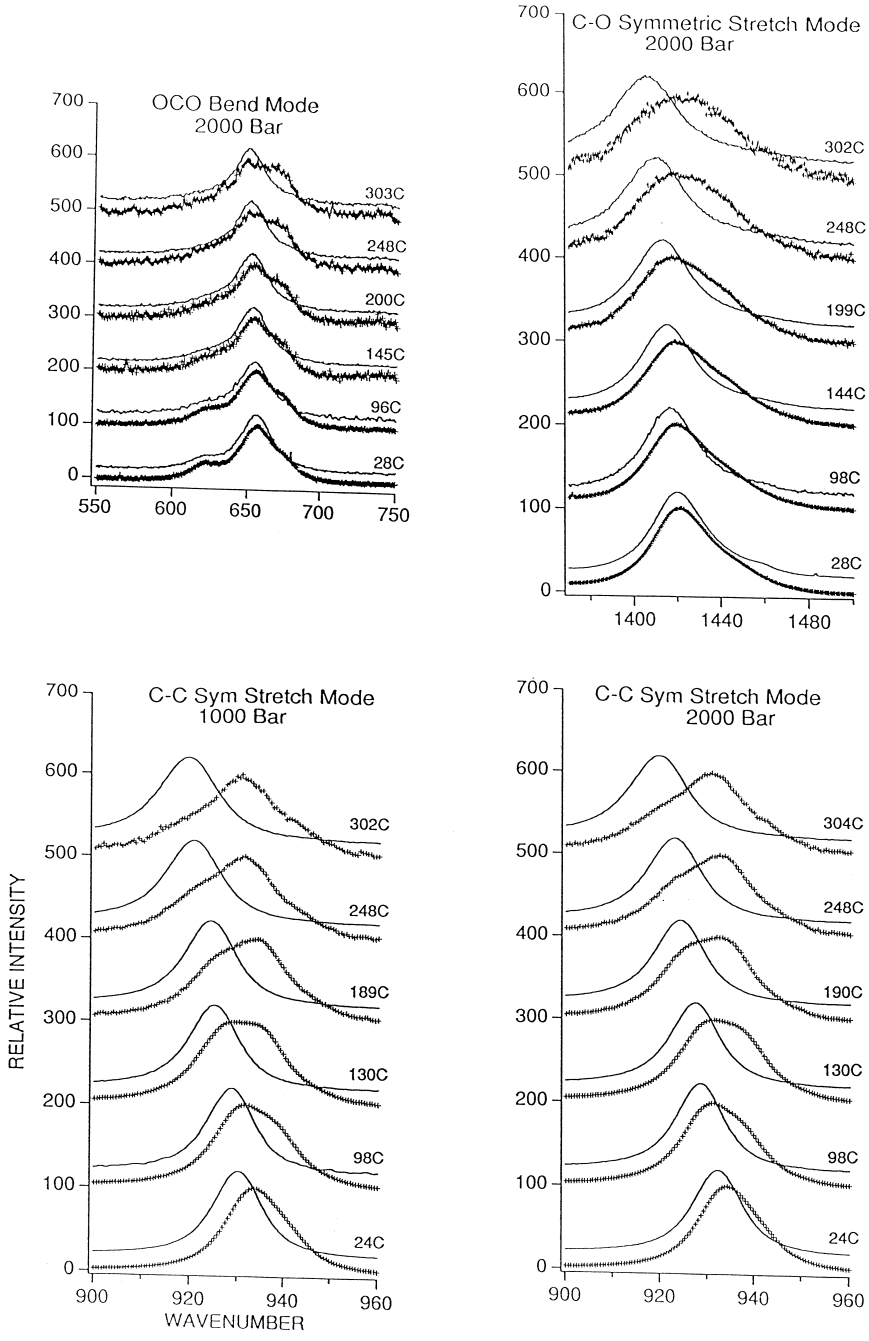


Fig. 6. Comparison of sodium acetate (solid lines) and calcium acetate (lines composed of markers) Raman bands for: (a) the OCO bending mode; (b) the C–O symmetric stretch mode; and (c) the C–C symmetric stretch mode. See text for additional details.

cations can be used to investigate ion association as a function of temperature and pressure. In the case of alkalis, these perturbations appear not to result in sufficiently large changes in the spectra of the ligand

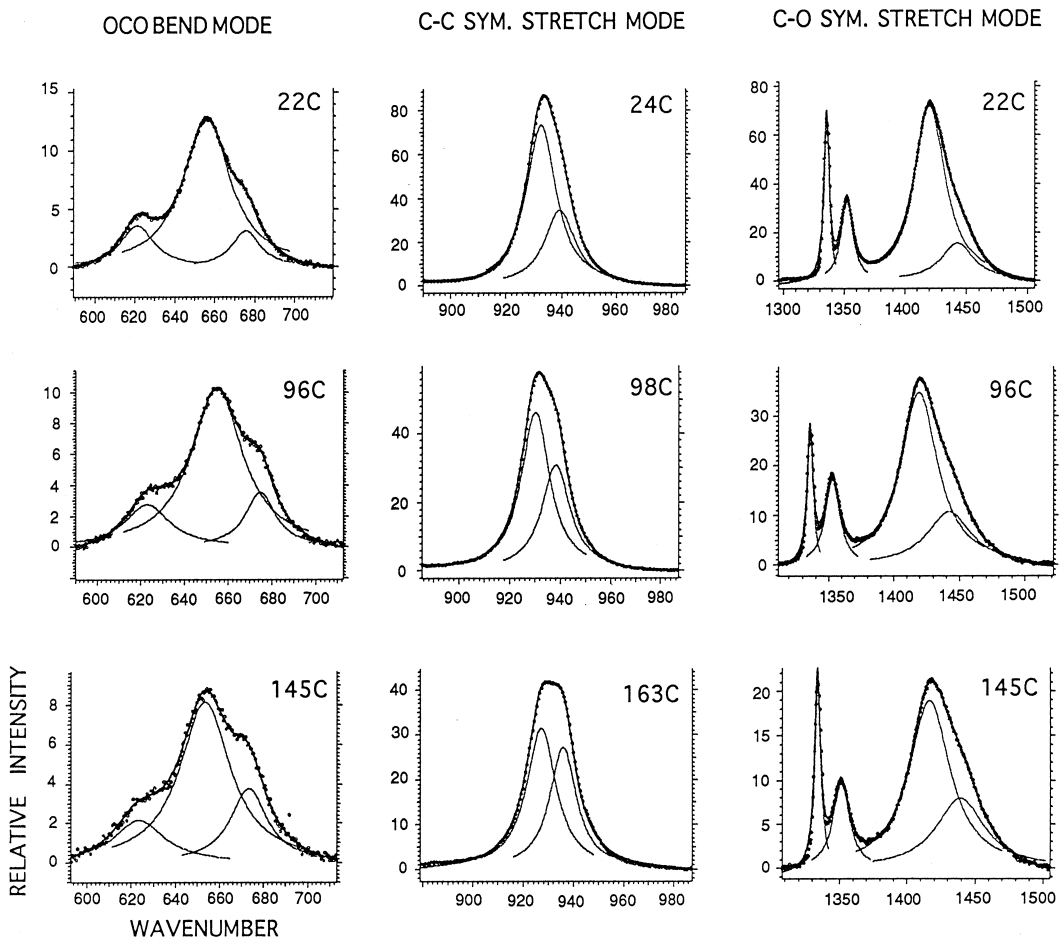


Fig. 7. Examples of spectral deconvolutions (calcium acetate) for the OCO bending mode, the C–C symmetric stretch mode and the C–O symmetric stretch mode at varying temperatures at 1000 bar pressure.

to enable the calculation of meaningful mass action constants describing the formation of ion pairs. In the study of potassium carbonate and bicarbonate solutions, for example (Frantz, 1998), both the frequencies and the half-widths of the internal vibrational modes of carbonate appeared to be unaffected by ion association with potassium ions as a function of temperature and pressure. Interactions between complex ligands and alkaline earths and transition metals, however, have been demonstrated to result in measurable changes in the spectra of the ligands. In the study of the Raman spectra of magnesium sulfate in aqueous solutions at temperatures from 25 to 550°C at pressures from 1 to 11 kbar (Frantz et al., 1994), the peak representing the S–O symmetric stretch (breathing mode) of the sulfate complex was seen to split as a result of ion association of magnesium and sulfate.

The differences in the spectra of the acetate ligand in calcium acetate solutions when compared to spectra in sodium acetate solutions and the changes in the calcium acetate spectra as a function of temperature, pressure, and concentration can be used both to establish the existence of calcium acetate complexes and to compute the association constant of $CaCH_3COO^+$. As demonstrated in Figs. 6 and 7, the bands representing the OCO bending mode, the C–C symmetric stretching mode, and the C–O symmetric stretching mode of the acetate ligand in sodium acetate solutions all split into two bands in calcium

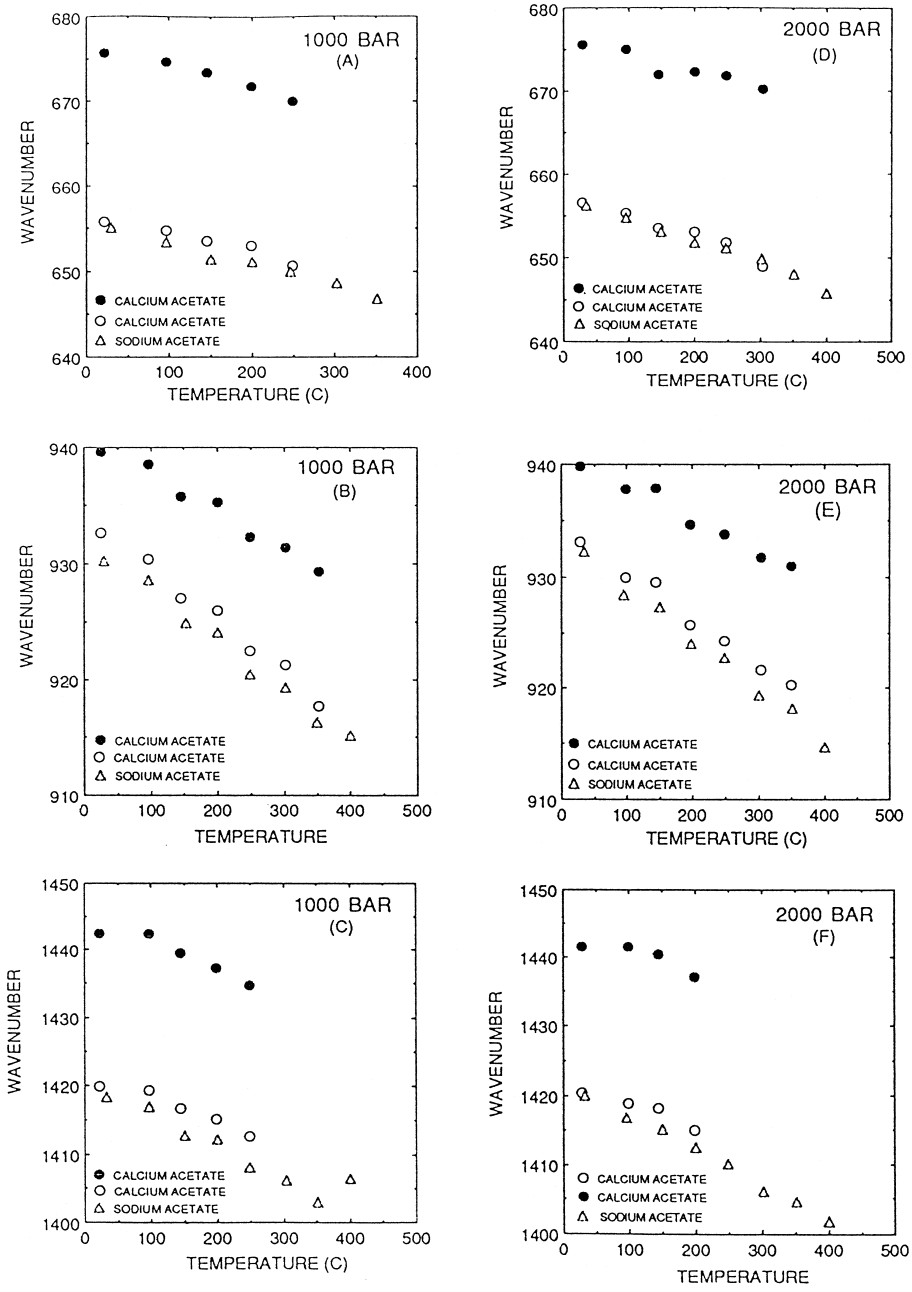


Fig. 8. Frequencies of deconvoluted spectral envelopes at 1000 and 2000 bar pressure. (A) and (D) refer to the OCO bending mode; (B) and (E), to the C–C symmetric stretch mode; (C) and (F), to the O–C symmetric stretch mode.

acetate solutions. As the internal modes of the acetate ligand are not measurably affected by the presence of sodium ions, the band positions for the acetate ions in sodium acetate solutions can represent both unbound acetate ions and sodium acetate ion-pairs. The lower-frequency components of the calcium acetate doublets, in each case, match the frequency of the corresponding single sodium acetate

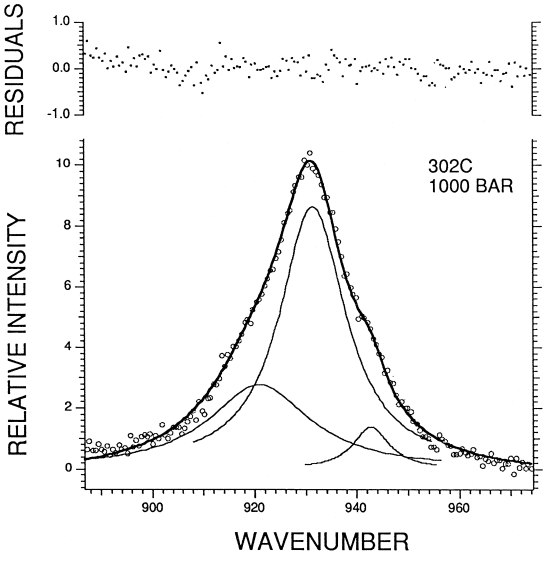


Fig. 9. Raman spectra of a 1 molal calcium acetate solution indicating the appearance of the neutral calcium acetate complex ($CaCH_3COO^{\cdot}$) at 302°C, 1000 bar.

bands (Fig. 8) and are therefore assumed to represent unbound acetate ions. The higher-frequency components would thus represent bound acetate. Assuming *stepwise* association constants for the species $Ca^{2+}$, $CaCH_3COO^+$, and $Ca(CH_3COO)_2^{\cdot}$:

$$Ca^{2+} + CH_3COO^- = CaCH_3COO^+ \quad (1)$$

$$CaCH_3COO^+ + CH_3COO^- = Ca(CH_3COO)_2^{\cdot} \quad (2)$$

the lower and higher frequency peaks in the doublets must represent $CH_3COO^-$ and $CaCH_3COO^+$ ions, respectively.

The concentration of an aqueous species can be related to the integrated area of a Raman band according to the following expression:

$$m_i = f_i A_i \quad (3)$$

where $m_i$ represents the molal concentration of the $i$th species; $A_i$, the area of the Raman peak representing the $i$th species; and $f_i$, the Raman scattering cross-section for the $i$th species. Dividing the concentration of bound acetate (representing $CaCH_3COO^+$) by that of unbound acetate ($CH_3COO^-$):

$$m_{CaCH_3COO^+}/m_{CH_3COO^-} = R\left(A_{CaCH_3COO^+}/A_{CH_3COO^-}\right) \quad (4)$$

where $R$ is the ratio of the Raman scattering cross of $f_{CaCH_3COO^+}$ over $f_{CH_3COO^-}$ respectively and $A_i$ represents the area of the $i$th species. Considering the mass balance expression for total acetate:

$$m_{CH_3COO(T)} = m_{CH_3COO^-} + m_{CaCH_3COO^+} + 2m_{Ca(CH_3COO)_2} \quad (5)$$

and assuming only minor concentrations of $Ca(CH_3COO)_2$, substitution of Eq. (4) into Eq. (5) yields an expression for the calculation of the molal concentration of $CH_3COO^-$:

$$m_{CH_3COO^-} = m_{CH_3COO(T)} / \left(1 + R\left(A_{CaCH_3COO^+}/A_{CH_3COO^-}\right)\right) \quad (6)$$

The molal concentration of $CaCH_3COO^+$ and $Ca^{2+}$ are calculated from:

$$m_{CaCH_3COO^+} = m_{CH_3COO(T)} - m_{CH_3COO^-} \quad (7)$$

and

$$m_{Ca^{2+}} = m_{Ca(T)} - m_{CaCH_3COO^+} \quad (8)$$

where $m_{Ca(T)}$ is the total concentration of calcium in the solution.

The relative areas of the Raman in the doublets corresponding to $CH_3COO^-$ and $CaCH_3COO^+$ are given in Table 1 for 0.1, 0.5, and 1.0 molal calcium acetate solutions. Errors corresponding to $\pm 1$ standard deviation of the deconvoluted areas are in parentheses after the corresponding values in Table 1. Assuming that the scattering cross-sections for the peaks in the doublets to be equal, the calculated concentrations of the species are presented in Table 2. In the case of the 1.0 molal calcium acetate solution, the relative areas are given for the OCO bending mode, the C–C symmetric stretch mode, and the C–O symmetric stretch mode. For the 0.1 and 0.5 molal solutions, only data for the C–C symmetric stretch mode were measured. Only the area ratios for the C–C symmetric stretch mode were used as deconvolutions of both the OCO bending mode and the C–O symmetric stretching mode involved peaks from overlapping modes. In the case of the OCO bending mode, the observation made earlier that the frequency of the out-of-plane rocking mode increased with increasing temperature may indicate

Table 2
Association constant calculations $Ca^{2+} + CH_3COO^- = CaCH_3COO^+$

| 1000 Bar $Ca(CH_3COO)_2$ total molality | Temp (°C) | Ratio $CaAc^+/Ac^-$ | $CH_3COO^-$ (molal) | $CaCH_3COO^+$ (molal) | $Ca^{2+}$ (molal) | Ionic strength | Log $\gamma_{Ca^{2+}}$ | Log $K$ |
|---|---|---|---|---|---|---|---|---|
| 1.0 | 53 | 0.52 | 1.32 | 0.68 | 0.32 | 1.64 | −0.66 | 0.87 (.07) |
| 1.0 | 79 | 0.61 | 1.24 | 0.76 | 0.24 | 1.48 | −0.69 | 1.09 (.07) |
| 1.0 | 98 | 0.73 | 1.16 | 0.84 | 0.16 | 1.31 | −0.73 | 1.40 (.09) |
| 0.5 | 50 | 0.32 | 0.76 | 0.24 | 0.26 | 1.01 | −0.64 | 0.74 (.06) |
| 0.5 | 73 | 0.28 | 0.78 | 0.22 | 0.28 | 1.07 | −0.68 | 0.67 (.04) |
| 0.5 | 104 | 0.37 | 0.73 | 0.27 | 0.23 | 0.96 | −0.69 | 0.90 (.04) |
| 0.5 | 128 | 0.45 | 0.69 | 0.31 | 0.19 | 0.88 | −0.72 | 1.09 (.04) |
| 0.5 | 152 | 0.69 | 0.59 | 0.41 | 0.09 | 0.69 | −0.74 | 1.61 (.06) |
| 0.5 | 175 | 0.85 | 0.54 | 0.46 | 0.04 | 0.58 | −0.77 | 2.07 (.11) |
| 0.1 | 121 | 0.11 | 0.18 | 0.02 | 0.08 | 0.26 | −0.59 | 0.70 (.10) |
| 0.1 | 151 | 0.26 | 0.16 | 0.04 | 0.06 | 0.22 | −0.59 | 1.22 (.10) |
| 0.1 | 179 | 0.29 | 0.15 | 0.05 | 0.05 | 0.21 | −0.61 | 1.35 (.11) |
| 0.1 | 199 | 0.26 | 0.16 | 0.04 | 0.06 | 0.22 | −0.67 | 1.32 (.09) |
| 0.1 | 230 | 0.90 | 0.11 | 0.09 | 0.01 | 0.11 | −0.58 | 2.81 (.69) |
| 2000 Bar $Ca(CH_3COO)_2$ total molality | Temp (°C) | Ratio $CaAc^+/Ac^-$ | $CH_3COO^-$ (molal) | $CaCH_3COO^+$ (molal) | $Ca^{2+}$ (molal) | Ionic strength | Log $\gamma_{Ca^{2+}}$ | Log $K$ |
| 1.0 | 53 | 0.44 | 1.39 | 0.61 | 0.39 | 1.79 | −0.71 | 0.76 (.07) |
| 1.0 | 75 | 0.50 | 1.33 | 0.67 | 0.33 | 1.67 | −0.76 | 0.93 (.06) |
| 1.0 | 98 | 0.57 | 1.28 | 0.72 | 0.28 | 1.55 | −0.79 | 1.09 (.06) |
| 1.0 | 129 | 0.77 | 1.13 | 0.87 | 0.13 | 1.26 | −0.83 | 1.59 (.10) |
| 0.5 | 49 | 0.27 | 0.79 | 0.21 | 0.29 | 1.07 | −0.62 | 0.60 (.06) |
| 0.5 | 72 | 0.27 | 0.79 | 0.21 | 0.29 | 1.07 | −0.66 | 0.63 (.05) |
| 0.5 | 104 | 0.29 | 0.77 | 0.23 | 0.27 | 1.05 | −0.67 | 0.70 (.03) |
| 0.5 | 127 | 0.37 | 0.73 | 0.27 | 0.23 | 0.96 | −0.70 | 0.91 (.04) |
| 0.5 | 152 | 0.47 | 0.68 | 0.32 | 0.18 | 0.86 | −0.72 | 1.14 (.04) |
| 0.5 | 175 | 0.55 | 0.64 | 0.36 | 0.14 | 0.79 | −0.76 | 1.34 (.04) |
| 0.5 | 201 | 0.77 | 0.57 | 0.43 | 0.07 | 0.63 | −0.77 | 1.84 (.09) |
| 0.1 | 121 | 0.06 | 0.19 | 0.01 | 0.09 | 0.28 | −0.65 | 0.50 (.17) |
| 0.1 | 152 | 0.10 | 0.18 | 0.02 | 0.08 | 0.26 | −0.58 | 0.66 (.08) |
| 0.1 | 179 | 0.39 | 0.15 | 0.05 | 0.05 | 0.20 | −0.57 | 1.41 (.18) |
| 0.1 | 200 | 0.30 | 0.15 | 0.05 | 0.05 | 0.21 | −0.61 | 1.36 (.13) |
| 0.1 | 231 | 0.55 | 0.13 | 0.07 | 0.03 | 0.16 | −0.59 | 1.49 (.08) |
| 0.1 | 253 | 0.72 | 0.12 | 0.08 | 0.02 | 0.13 | −0.60 | 2.60 (.37) |

that additional peak(s) may contribute to the spectral envelope but not be resolvable. With respect to the envelope containing the symmetric C–O stretch, the presence of the antisymmetric $CH_3$ deformation complicates deconvolution. In addition, since the oxygens in the OCO bend and C–O stretching modes are intimately involved with the association of the acetate ligand with calcium, the assumption that the ratio of the scattering coefficients being unity is much less robust. Mass action constants were calculated for Eq. (1):

$$\text{Log } K = a_{CaCH_3COO^+}/a_{Ca^{2+}}a_{CH_3COO^-} \quad (9)$$

Assuming the activity coefficients of $CaCH_3COO^+$ ($\gamma_{CaCH_3COO^+}$) and $CH_3COO^-$ ($\gamma_{CH_3COO^-}$) are equal (assuming the ion size parameters for the acetate ion and the calcium acetate ion-pair in the extended Debye–Huckel expression are approximately equal):

$$\text{Log } K = \left[m_{CaCH_3COO^+}/m_{Ca^{2+}}m_{CH_3COO^-}\right]\left[1/\gamma_{Ca^{2+}}\right] \quad (10)$$

where $\gamma_{Ca^{2+}}$ is the activity coefficient of calcium ion. The molal activity coefficient of calcium ion was computed using the ''B-dot'' equation as described in the work of Helgeson (1969). Debye–Huckel parameters were obtained from Helgeson and Kirkham (1974); the ion size parameter, from Klotz (1964). The computed ionic strengths, activity coefficients of calcium ion, and mass action constants for the three concentrations at 1000 and 2000 bar are given in Table 2. The numbers in parentheses listed after the values of Log $K$ in Table 2 represent the errors in the calculated equilibrium constants due to the errors in the measurement of peak area (listed in Table 1). The calculated values for the logarithm (base 10) of the association constant (along with the associated errors) are shown as a function of inverse temperature ($K$) in Fig. 10 for 1000 and 2000 bar. The dashed lines represent an uncertainty of $\pm 1$ standard deviation in the fitted line. While agreement is quite good, there is a reasonably small but systematic variation of the values of Log $K$ with concentration. The origin of this trend is unknown. Values of activity coefficients, the Raman scattering coefficient ratio, line shapes used in spectral deconvolutions, etc. are all possibilities but, without further information, the cause of this uncertainty remains uncertain.

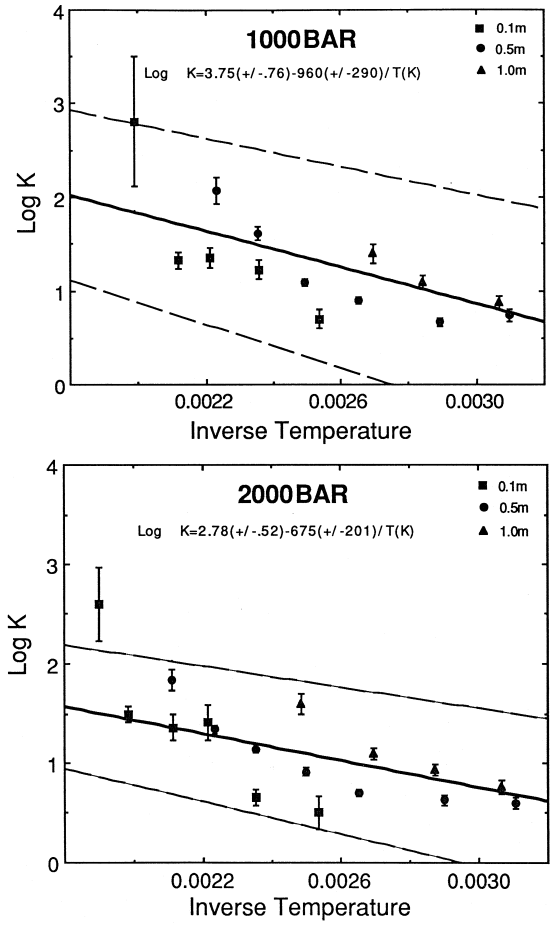


Fig. 10. Computed association constants at both 1000 and 2000 bar pressure for the equilibrium: $Ca^{2+} + CH_3COO^- = CaCH_3COO^+$. Error bars are plotted for individual data points. The solid lines represent weighted regressions of the data. The dashed lines represent an error of $\pm 1$ standard deviation for these fitted lines.

In Fig. 11, the values of the logarithm of the association constant at 1000 and 2000 bar (this work) and the experimentally determined value at 500 bar (Seewald and Seyfried, 1991) at 200°C are plotted as a function of the logarithm of the density of water. Plots such as these have been demonstrated to be linear for association constants (Quist and Marshall, 1968). The data appear to be reasonably consistent. The errors for the 1000 bar and 2000 bar data represent the errors for the fitted line of the association constant shown in Fig. 10. No errors are available for the data of Seewald and Seyfried (1991) but

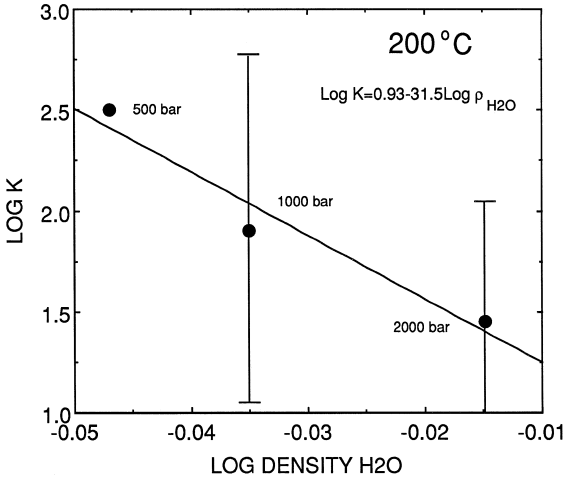


Fig. 11. Comparison of the results of these experiments at 1000 and 2000 bar with the result of Seewald and Seyfried (1991) at 500 bar. Error bars representing $\pm 1$ standard deviation of the fitted line shown in Fig. 10 are plotted for these experiments. No errors were provided by Seewald and Seyfried (1991). The line is fitted through the experimental data both of this work and that of Seewald and Seyfried (1991).

are probably large due to the fact that retrieval of their data involved the simultaneous solution of a number of mass action expressions. Significant uncertainty exists for each of the mass action constants associated with these expressions. Shock and Koretsky (1993) theoretically estimated values of the logarithm of the mass action constant. Their values at 200°C are 2.27, 2.16, and 2.02 at 500, 1000, and 2000 bar, respectively. Their estimates appear to show a reduced effect of pressure on the values of the association constants. Calculation of species distributions and mass action constants were restricted to temperature–pressure conditions at which the relative area of the peak representing $CaCH_3COO^+$ was less than that of the peak representing $CH_3COO^-$. At higher temperature conditions at which the area of calcium acetate exceeds that of acetate, it is assumed that the concentration of the neutral species $Ca(CH_3COO)_2^{\circ}$ is becoming important. This assump-

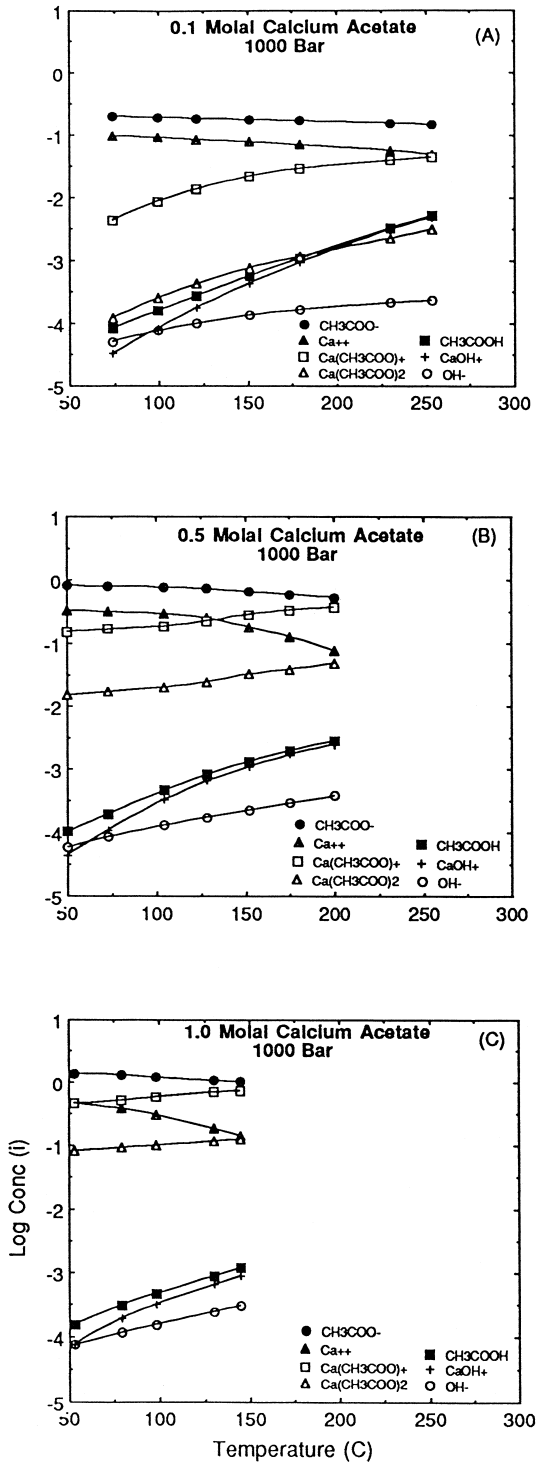


Fig. 12. Distribution of aqueous species of calcium acetate solutions as a function of temperature at 1000 bar pressure. (A) 0.1 molal calcium acetate solution; (B) 0.5 molal calcium acetate solution; and (C) 1.0 molal calcium acetate solution.

tion is consistent with the appearance of a third peak in the symmetric C–C stretch envelope at 248°C at 1000 bar and 304°C at 2000 bar for the experiments performed on 1.0 molal calcium acetate solutions (Fig. 9; Table 1).

## 5. Discussion

In order to model the chemical evolution of calcium acetate solutions as they are subjected to increasing temperature and pressure in the experiments discussed above, the chemical compositions of these fluids were computed using available experimentally and theoretically determined thermodynamic data. The principal source for these data was the data base for *SUPCRT92* (Johnson et al., 1992) updated with theoretically derived data from Shock et al. (1997). Association constants for the equilibria $Ca(CH_3COO)^+ + CH_3COO^- = Ca(CH_3COO)_2^\circ$ and $CaOH^+ + OH^- = Ca(OH)_2^\circ$ were assumed to be identical to those of the equilibria $Na^+ + Cl^- = NaCl^\circ$. This is justified by the relative similarity of these constants for a variety of salts including the first association constants of $CaCl_2$ and $MgCl_2$ (Frantz and Marshall, 1982). Values for the reaction $Ca^{2+} + CH_3COO^- = Ca(CH_3COO)^+$ were taken directly from Table 2 rather than from regressions of the data due to the dependence of the values of Log $K$ on concentration. These data were used to compute the distributions of aqueous species for 0.1, 0.5, and 1.0 molal calcium acetate solutions as a function of temperature and pressure (Fig. 12). Calculations were performed using the program listed in the Appendix of Frantz et al. (1981). Activity coefficients were computed using the ''B-dot'' equation as described in the work of Helgeson (1969). The results, shown in Fig. 12, indicate that the experimental solutions were quite basic with the concentration of hydroxide increasing with increasing temperature and calcium acetate concentration. The calcium hydroxide species, $CaOH^+$ and $Ca(OH)_2^\circ$, are present in much smaller concentrations than the calcium acetate complexes and thus would be expected not to interfere with the interpretation of this spectral study. The species $Ca(OH)_2^\circ$, not shown in Fig. 12, occurs at concentrations less than $1.0 \times 10^{-7}$ molal. Acetic acid appears to occur at concentrations several orders of magnitude less than that of acetate or $Ca(CH_3COO)^+$ and thus would not be expected to be resolvable in the Raman spectra. The neutral species, $Ca(CH_3COO)_2^\circ$, appears to be increasing in concentration with both increasing temperature and total calcium acetate concentration. Inspection of the trends in Fig. 12 indicate that it would be likely to expect the appearance in the Raman spectra of the neutral complex in 1.0 molal solutions at the higher experimental temperatures *of the study* as shown in Fig. 9. Appearance of this species would not be likely at lower total calcium acetate concentrations.

## Acknowledgements

The project was supported by the Carnegie Institution of Washington and a grant from the Centre National de la Recherche Scientifique through its Programme International de Cooperation Scientifique (PICS #142).*[SB]*

## References

Drummond, S.E., Palmer, D.A., 1986. Thermal decarboxylation of acetate: Part II. Boundary conditions for the role of acetate in the primary migration of natural gas and the transportation of metals in hydrothermal systems. Geochim. Cosmochim. Acta 50, 825–833.

Ellis, A.J., 1963. The ionization of acetic, propanoic, *n*-butyric, and benzoic acid in water, from conductance measurements up to 225°C. J. Chem. Soc. 1963, 2299–2310.

Frantz, J.D., 1981. High-pressure, high-temperature optical cell for Raman spectroscopy. Carnegie Inst. Washington, Year Book 80, 406–408.

Frantz, J.D., 1998. Raman spectra of potassium carbonate and bicarbonate aqueous fluids at elevated temperatures and pressures: comparison with theoretical simulations. Chem. Geol., in press.

Frantz, J.D., Marshall, W.L., 1982. Electrical conductance and ionization constants for calcium chloride and magnesium chloride in aqueous solutions at temperatures to 600°C and pressures to 4000 bars. Am. J. Sci. 282, 1666–1693.

Frantz, J.D., Popp, R.K., Boctor, N.Z., 1981. Mineral–solution equilibria: V. Solubilities of rock-forming minerals in supercritical fluids. Geochim. Cosmochim. Acta 45 (1), 69–77.

Frantz, J.D., Dubessy, J., Mysen, B.O., 1993. An optical cell for Raman spectroscopic studies in supercritical fluids and its application to the study of water to 500°C and 2000 bar. Chem. Geol. 106, 9–26.

Frantz, J.D., Dubessy, J., Mysen, B.O., 1994. Ion-pairing in aqueous $MgSO_4$ solutions along an isochor to 500°C and 11

kbar using Raman spectroscopy in conjunction with the diamond-anvil cell. Chem. Geol. 116, 181–188.

Giordano, T.H., 1989. Anglesite ($PbSO_4$) solubility in acetate solutions: the determination of stability constants for lead acetate complexes to 85°C. Geochim. Cosmochim. Acta 53, 359–366.

Giordano, T.H., 1993. Metal transport in ore fluids by organic ligand complexation. In: Pittman, E.D., Lewan, M.D. (Eds.), Organic Acids in Geological Processes. Springer-Verlag, New York, NY, 482 pp.

Helgeson, H.C., 1969. Thermodynamics of hydrothermal systems at elevated temperatures and pressures. Am. J. Sci. 267, 729–804.

Helgeson, H.C., Kirkham, D.H., 1974. Theoretical prediction of the thermodynamic behavior of aqueous electrolytes at high pressures and temperatures: II. Debye–Huckel parameters for activity coefficients and relative partial molal properties. Am. J. Sci. 274, 1199–1261.

Johnson, J.W., Oelkers, E.H., Helgeson, H.C., 1992. SUPCRT92: a software package for calculating the standard molal thermodynamic properties of minerals, gases, aqueous species, and reactions from 1 to 5000 bar and 0 to 1000°C. Comput. Geosci. 18 (7), 899–947.

Kaklhana, M., Kotaka, M., Okamoto, M., 1983. Vibrational analysis of acetate ion molecules and estimation of equilibrium constants for their hydrogen isotopic exchange reactions. J. Phys. Chem. 87, 2526–2535.

Kharaka, Y.K., Carothers, W.W., Rosenbauer, R.J., 1983. Thermal decarboxylation of acetic acid: implications for origin of natural gas. Geochim. Cosmochim. Acta 47, 397–402.

Klotz, I.M., 1964. Chemical Thermodynamics. W.A. Benjamin, New York, NY, 468 pp.

Long, D.A., 1977. Raman Spectroscopy. McGraw-Hill, New York, NY, 276 pp.

Palmer, D.A., Drummond, S.E., 1986. Thermal decarboxylation of acetate: Part I. The kinetics and mechanism of reaction in aqueous solution. Geochim. Cosmochim. Acta 50, 813–823.

Palmer, D.A., Drummond, S.E., 1988. Potentiometric determination of the molal formation constants of ferrous acetate complexes in aqueous solutions to high temperatures. J. Phys. Chem. 92, 6796–6800.

Quist, A.S., Marshall, W.L., 1968. Electrical conductances of aqueous sodium chloride solutions from 0 to 800° and to pressures of 4000 bars. J. Phys. Chem. 72, 684–703.

Seewald, J.S., Seyfried, W.E., 1991. Experimental determination of portlandite solubility in $H_2O$ and acetate solutions at 100–350°C and 500 bars: constraints on calcium hydroxide and calcium acetate complex stability. Geochim. Cosmochim. Acta 55, 659–669.

Semmler, J., Irish, D.E., 1988. Vibrational spectral studies of solutions at elevated temperatures and pressures: 9. Acetic acid. J. Sol. Chem. 17, 805–824.

Semmler, J., Irish, D.E., Ozeki, T., 1990. Vibrational spectral studies of solutions at elevated temperatures and pressures: 12. Magnesium acetate. Geochim. Cosmochim. Acta 54, 947–954.

Shock, E.L., 1993. Application of thermodynamic calculations to geochemical processes. In: Pittman, E.D., Lewan, M.D. (Eds.), Organic Acids in Geological Processes. Springer-Verlag, New York, NY, 482 pp.

Shock, E.L., Koretsky, C.M., 1993. Metal-organic complexes in geochemical processes: calculation of standard partial molal thermodynamic properties of aqueous acetate complexes at high pressures and temperatures. Geochim. Cosmochim. Acta 57, 4899–4922.

Shock, E.L., Sassani, D.C., Willis, M., Sverjensky, D.A., 1997. Inorganic species in geologic fluids: correlations among standard molal thermodynamic properties of aqueous ions and hydroxide complexes. Geochim. Cosmochim. Acta 61 (5), 907–950.

Spohn, P.D., Brill, T.B., 1989. Raman spectroscopy of the species in concentrated aqueous solutions of $Zn(NO_3)_2$, $Ca(NO_3)_2$, $Cd(NO_3)_2$, $LiNO_3$, and $NaNO_3$ up to 450°C and 30 MPa. J. Phys. Chem. 93, 6224–6231.

Sverjensky, D.A., 1984. Oil field brines as ore-forming solutions. Econ. Geol. 79, 23–37.

Yang, M.M., Crerar, D.A., Irish, D.E., 1989. A Raman spectroscopic study of lead and zinc acetate complexes in hydrothermal solutions. Geochim. Cosmochim. Acta 53, 319–326.